Published in final edited form as:
Biochemistry. 2010 November 30; 49(47): 10072–10080. doi:10.1021/bi100885v.

Pivotal Roles of Three Conserved Carboxyl Residues of NuoC (30k) Segment in the Structural Integrity of Proton-translocating NADH-Quinone Oxidoreductase (NDH-1) from *Escherichia coli*[#]

Norma Castro-Guerrero[†], **Prem Kumar Sinha**[†], **Jesus Torres-Bacete**, **Akemi Matsuno-Yagi**, and **Takao Yagi**[*]
Department of Molecular and Experimental Medicine, The Scripps Research Institute, 10550 North Torrey Pines Road, La Jolla, California 92037

Abstract

The prokaryotic proton-translocating NADH-quinone oxidoreductase (NDH-1) is an L-shaped membrane-bound enzyme that contains 14 subunits (NuoA-NuoN/Nqo1-Nqo14). All subunits have their counterparts in the eukaryotic enzyme (complex I). NDH-1 consists of two domains: the peripheral arm (NuoB,C,D,E,F,G, and I) and the membrane arm (NuoA,H,J,K,L,M, and N). In *Escherichia coli* NDH-1 the hydrophilic subunits NuoC/Nqo5/30k and NuoD/Nqo4/49k are fused together in a single polypeptide as the NuoCD subunit. The NuoCD subunit is the only subunit that does not bear a cofactor in the peripheral arm. While some roles for inhibitor- and quinone-association have been reported for the NuoD segment, structural and functional roles of the NuoC segment remain mostly elusive. In the current work, 14 highly conserved residues of the NuoC segment were mutated and 21 mutants were constructed using the chromosomal gene manipulation technique. From the enzymatic assays and immunochemical and blue-native gel analyses, it was found that residues Glu-138, Glu-140, and Asp-143 that are anticipated to be in the third α-helix are absolutely required for the energy-transducing NDH-1 activities and the assembly of the whole enzyme. Together with available information for the hydrophobic subunits, it is proposed that Glu-138, Glu-140, and Asp-143 of the NuoC segment may have a pivotal role in structural stability of NDH-1.

The proton-translocating NADH-quinone oxidoreductase (NDH-1 for bacteria and complex I for mitochondria) catalyzes the reduction of Q by using NADH as an electron donor coupled to the translocation of protons across the inner mitochondrial or the bacterial cytoplasmic membrane (1–3). Complex I is the largest enzyme complex of the respiratory chain; in case of the bovine enzyme, it is composed of 45 different subunits (4). In contrast, the bacterial NDH-1 is generally composed of 14 subunits which are homologues of the 14 subunits that comprise the central core of the mitochondrial enzyme (1,5,6). Earlier structural studies (7) showed that NDH-1, like complex I, consists of two domains: One is a hydrophobic domain composed of 7 subunits related to the proton translocation process and the other is a hydrophilic domain (peripheral arm) that hosts another 7 subunits containing

[#]This work was supported in part by CONACyT-MEXICO 76103 (N.C.-G.) and NIH R01GM033712 (A.M.-Y. and T.Y.)

[*]Corresponding author: yagi@scripps.edu; Tel, 858-784-8094; Fax, 858-784-2054.
[†]These two authors contributed eaqually to this work.

Supporting Information Available

Oligonucleotides used for the cloning and mutagenesis of *E. coli* nuoCD gene; Sequence alignment of NuoC segment from *E. coli* NDH-1 with its homologues from other organisms; A cartoon representation of the 3-D model of the NuoCD subunit of *E. coli* NDH-1 obtained by homology modeling on the crystallographic data of *T. thermophilus* enzyme; Visualization of the NuoC-NuoD interface in the NuoCD subunit of *E. coli* NDH-1 showing possible ionic interactions between residues Glu-140 and Arg-560 or Glu-140 and Arg-600. This material is available free of charge via the Internet at http://pubs.acs.org.

all the redox components (flavin mononucleotide and 8 to 9 iron sulfur clusters) (2,7–13). Crystallographic analysis of the peripheral arm of *Thermus thermophilus* NDH-1 greatly advanced our knowledge about its structure (10,11).

Escherichia coli NDH-1 possesses 13 subunits (NuoA to NuoN) encoded by the *nuo* operon. The peripheral arm of the *E. coli* enzyme has 6 subunits (NuoB, CD. E, F, G and I) (14). In most organisms, NuoCD is separated into 2 subunits with the NuoC segment being a homolog of *Rhodobacter capsulatus* NuoC (15)/*T. thermophilus* Nqo5 (16)/bovine 30k (1)and the NuoD segment a homolog of *Rhodobacter capsulatus* NuoD (15)/*T. thermophilus* Nqo4 (16)/bovine 49k (1). NuoCD is the only subunit in the peripheral arm that does not bear a cofactor. Several observations have been reported that subunit NuoD/Nqo4/49k is involved in the binding and reduction of Q (17–19). Information about the role of the NuoC segment remains limited. The sequence comparison of the NuoC segment of *E. coli* NuoCD with its counterparts in diverse organisms revealed the presence of highly conserved residues. To gain insight into the role of NuoC/Nqo5/30k, we constructed site-directed mutants of the residues conserved in the NuoC segment of *E. coli* NDH-1 by taking advantage of the chromosomal DNA manipulation technique that we have successfully adopted for characterization of various hydrophobic subunits of the membrane domain (20–25). Use of bacterial systems has advantages for the structural and functional study of complex I/NDH-1 and is applicable to both hydrophobic core subunits and peripheral core subunits (6,14,15,26). Absence of the so-called "accessory subunits" provides a simpler system to handle. Also, unlike the mitochondrial system, there are no potential complications associated with import of proteins and cofactors that requires ATP and membrane potential. Possible engagement of the NuoC segment in the architecture of NDH-1 is discussed.

EXPERIMENTAL PROCEDURES

Materials

The pGEM-T Easy Vector was from Promega (Madison, WI). The QuikChange®II XL site-directed mutagenesis kit and the Herculase®-enhanced DNA polymerase were obtained from Stratagene (Cedar Creek, TX). Materials for PCR product purification, gel extraction and plasmid preparation were from Qiagen (Valencia, CA). Endonucleases were from New England Biolabs (Beverly, MA). The gene replacement vector, pKO3, was kindly provided by Dr. George M. Church (Harvard Medical School, Boston, MA). The BCA protein assay kit and SuperSignal West Pico chemiluminescent substrate were from Pierce (Rockford, IL). Goat anti-rabbit IgG horseradish peroxidase conjugate was from GE Healthcare (Piscataway, NJ). NADH, dNADH, DB, and chemicals were from Sigma-Aldrich (St. Louis, MO). *p*-nitroblue tetrazolium was from EMD Biosciences (La Jolla, CA). Oxonol VI and ACMA were from Invitrogen (Carlsbad, CA). Antibodies against *E. coli* NDH-1 subunits NuoB, NuoCD, NuoE, NuoF, NuoG and NuoI were obtained previously in our laboratory (24). Cap-40 was a generous gift from Dr. Hideto Miyoshi (Kyoto University, Kyoto, Japan) (27). Oligonucleotides were synthesized by Valuegene (San Diego, CA). All other materials were reagent grade and were obtained from commercial sources.

Cloning and Mutagenesis of the E. coli nuoCD gene

Cloning and mutagenesis for the *E. coli nuoCD* gene were performed as described previously (20–24,28) and summarized in Fig. 1. Sequence alignment of several organisms was carried out to identify the conserved residues of the NuoC segment (Fig. S1). The first 193 amino acid residues of the NuoCD subunit have been extracted on the basis of alignment to the sequences of the Nqo5/NuoC subunit and homologues from several organisms. We refer to this part as the NuoC segment in this work. Primer sequences

designed to insert point mutations in the selected residues are given in Table S1. The DNA fragment encoding the NuoC segment plus 1-kb upstream and downstream was amplified by PCR from *E. coli* DH5α using primers A and D. The constructs harbored a *Bam*HI restriction site (Fig. 1). The amplified product was cloned in pGEM-T Easy vector and finally subcloned into the integration vector pKO3 resulting in plasmids named pGEM/*nuoC* and pKO3/*nuoC*, respectively, as shown in Fig. 1(a). A 1-kb DNA segment upstream with the 5'-sequence of the *nuoCD* gene was amplified by PCR using primers A and B, generating the fragment *nuoC-U*. Another 1 kb DNA segment downstream with the 3'-sequence of *nuoCD* gene was amplified using primers C and D, generating the fragment *nuoC-D*. Both fragments were cloned in the pGEM-T Easy vector. The spectinomycin-encoding gene (*spc*) was obtained by amplification from transposon Tn554 of *Staphylococcus aureus* using primers E and F, both containing the *Hind*III restriction site (Fig. 1(b)). The *spc* fragment obtained was cloned in the pGEM-T Easy vector and finally inserted between the fragments *nuoC-U* and *nuoC-D* utilizing the *Hind*III restriction sites. The complete construction was assembled in the pKO3 vector generating pKO3/*nuoC* (*spc*) plasmid with the help of *Bam*HI restriction sites (Fig. 1(c)). To introduce point mutations in the *nuoCD* gene, the plasmid pGEM/*nuoC* was used as a template along with the primers carrying the desired mutation and the QuikChange®II-XL site-directed mutagenesis kit. The mutated fragments were then inserted into the pKO3 plasmid utilizing the *Bam*HI restriction sites, generating the pKO3/*nuoC* (mutant). All sequences were confirmed by DNA sequencing.

Preparation of the nuoC segment Knock-out and Mutant Cells

E. coli strain MC4100 (*F*⁻, *araD139*, Δ*(arg F-lac) U169, ptsF25, relA1, flb5301, rpsL 150*.λ⁻) was used to generate knockout (KO-C) and site-specific mutations of the NuoC segment in the *nuoCD* gene using the pKO3 system (29) with a minor modification as described previously by Kao *et al*. (20). The KO-C mutant was constructed by replacement of the NuoC segment of the *nuoCD* gene in the NDH-1 operon for the *nuoC* (*spc*) fragment inserted in the pKO3 plasmid. In the subsequent steps KO-C competent cells were made in order to generate the mutants using the pKO3/*nuoC* (mutant) plasmids for the recombination process. A control KO-C-rev (KO-C-revertant) was generated in the same way using the pKO3/*nuoC* carrying the wild-type *nuoCD* gene instead of pKO3/*nuoC* (mutant) for the recombination process. The correct introduction of point mutations in the chromosome was verified by direct DNA sequencing.

Bacterial Growth and membrane preparation

The *E. coli* membrane preparation was made as reported previously (22–24). Briefly, cells were grown in 250 ml of Terrific Broth medium at 37 °C until A_{600} of 2. Then the cells were harvested by centrifugation at 5,800 × g for 10 minutes and frozen at −80°C. The membrane vesicles were prepared according to the method described previously (20–22).

Activity measurements

Analysis of the *E. coli* NDH-1 NuoC segment mutants activity was carried out according to the methods described previously (20). The reactions were performed at 30 °C using dNADH as substrate in a SLM DW-2000 spectrophotometer. dNADH-$K_3Fe(CN)_6$ reductase activity was performed at 30 °C with 80 μg of protein/ml of membrane samples in 10 mM potassium phosphate (pH 7.0), 1 mM EDTA, 10 mM KCN and 1 mM $K_3Fe(CN)_6$. The reactions were started by the addition of 150 μM dNADH and the measurements were followed at 420 nm. The dNADH-DB reductase activity was performed under similar conditions, except that $K_3Fe(CN)_6$ was replaced by 60 μM DB and the measurements were followed at 340 nm. The dNADH oxidase activity was measured using the same conditions, but without addition of KCN or DB in the reaction buffer. Ten μM Cap-40 (27) was used for

monitoring the inhibition of energy-transducing dNADH-DB reductase and dNADH oxidase activities. The extinction coefficients used for activity calculations were ε_{340}=6.22 $mM^{-1}cm^{-1}$ for dNADH and ε_{420}=1.00 $mM^{-1}cm^{-1}$ for $K_3Fe(CN)_6$.

The membrane potential generated by the NDH-1 mutants was monitored optically using oxonol VI as reporter (21). The reactions were carried out at 30 °C with 0.33 mg of protein/ml of membrane samples in 50 mM MOPS (pH 7.3), 10 mM $MgCl_2$ and 50 mM KCl buffer containing 2 μM oxonol VI. The reactions were started with the addition of 200 μM dNADH and the absorbance changes at 630-603 nm were recorded. Proton pump activity was followed by ACMA fluorescence quenching as described by Amarneh and Vik (30). As a respiratory substrate, 200 μM dNADH was added in the reaction mixtures. 2 μM FCCP was used to dissipate the membrane potential and the proton gradient across the membranes.

Western blotting analysis and Blue-Native gel electrophoresis

The contents of the NDH-1 subunits in the NuoC segment mutants were analyzed using antibodies against NuoB, NuoCD, NuoE, NuoF, NuoG and NuoI subunits in a Western blot experiment. The assembly of NDH-1 in NuoC segment mutants was evaluated by Blue-Native PAGE (BN-PAGE) as reported by Schägger and von Jagow (31) with minor modifications (23). The NADH dehydrogenase activity staining of the BN-PAGE gels was done with a 1 h incubation at 37 °C in the presence of 2.5 mg/mL of *p*-nitroblue tetrazolium and 150 μM NADH. The reaction was stopped with 7% acetic acid.

Other Analytical Procedures

Protein concentrations were determined using the BCA™ protein assay kit (Pierce) with bovine serum albumin as a standard according to the manufacturer's instructions. Any variations from the procedures and details are described in the figure legends.

3-D Structure modeling

A 3D model of the *E. coli* NuoCD subunit was constructed using a homology modeling program MODELLER 9v8 (32). The coordinates for the *T. thermophilus* NDH-1 (3IAS) were used as a template. The alignment file consisted of sequences from the target (*E. coli* NuoCD) and the template (*T. thermophilus* Nqo5 and Nqo4 concatenated). Chain 5 and chain 4 of the *T. thermophilus* NDH-1 coordinates were extracted (in this order) and used as a template structure file. Sequence alignment was made using the CLUSTAL W program (33). The 3-D structure was visualized and analyzed with PyMOL v1.2 (34). Measurements and appearance manipulation were carried out with the Wizard tools available in the software.

RESULTS

Sequence analysis of the NuoC segment in E. coli NDH-1

There are at least 14 conserved amino acid residues in the *E. coli* NuoC segment and its homologues: Ser-104, Ala-134, Glu-138, Arg-139, Glu-140, Asp-143, Gly-146, Phe-149, Arg-156, Gly-166, His-167, Pro-168, Lys-171, and Pro-182 (Fig. S1). According to the 3D structural model of *Thermus* NDH-1, the Nqo5 subunit contains five helices and five β-sheets (10,11). Taking advantage of a relatively high amino acid sequence similarity between the *Thermus* and *E. coli* NDH-1, we constructed a 3-D structural model of the *E. coli* NuoCD subunit based on crystallographic data of the *Thermus* Nqo4 and Nqo5 subunits (10,11) using homology modeling software MODELLER (32). A reasonably well-fitting model of the *E. coli* subunit was obtained (Fig. S2). Most of the conserved residues are located either in the third α-helix (Ala-134, Glu-138, Arg-139, Glu-140, Asp-143) or in the surrounding area (Gly-146, Phe-149, Arg-156, Gly-166, His-167, Pro-168) as displayed in

Fig. 2. We constructed mutants of all 14 highly conserved residues of the NuoC segment using chromosomal gene manipulation technique and used these mutants for the characterization of the individual residues.

Effects of NuoC Segment Mutation on the NDH-1 Activities

E. coli contains an alternative NADH dehydrogenase (NDH-2) in addition to NDH-1. To measure the activities derived solely from NDH-1, we used dNADH as the substrate because NDH-2 cannot catalyze dNADH oxidation (35). We conducted three types of assays, namely, dNADH oxidase activity, dNADH-Q oxidoreductase activity, and dNADH dehydrogenase (dNADH-$K_3Fe(CN)_6$ reductase) activity, to assess the effects of the mutations.

Since the point mutations were checked by DNA sequencing of the *nuoCD* gene and its flanking regions only, we could not rule out a possibility that the gene replacement process might have altered other genes. To address this issue, we reintroduced the native NuoC segment into the knock-out (KO-C) mutant following the same procedure used to generate point mutants (KO-C-rev mutant). As shown in Table 1, the KO-C-rev mutant displayed properties indistinguishable from the wild-type strain in all enzymatic activities tested. Furthermore, immunoblotting results of the membranes with antibodies specific to the peripheral subunits (Fig. 3) and the pattern of the NADH dehydrogenase staining in the BN-PAGE of the membranes (Fig. 4) exhibited no difference between the KO-C-rev mutant and the wild-type strains. This proved that the procedure used to introduce point mutations in the chromosome did not cause any modification at the protein level that affected the NDH-1 respiratory function. The KO-C-rev mutant, thus, could serve as an appropriate reference strain in addition to the original MC4100 wild-type strain.

We first tested all mutants constructed for the dNADH-$K_3Fe(CN)_6$ reductase assay (Table 1). The activity of the KO-C mutant was 36% of the wild type. Point mutants E138A, E138D, E138Q, E140A, E140Q and D143A showed suppressed activities varying from 30 to 50% of the control. D143N showed a moderate decrease with approximately 70% of the control. In contrast, no or little activity loss was observed with mutants E140D, D143E, S104A, A134S, R139A, G146A, F149A, R156A, G166A, H167A, P168A, K171A, K171R, and P182A. We then measured the dNADH oxidase activity. In those mutants that had no significant loss in the dNADH-$K_3Fe(CN)_6$ reductase activity, the dNADH oxidase activity was also not affected, suggesting that the mutated residues are not essential. We note that the dNADH oxidase activity and dNADH-Q oxidoreductase activities behaved in a similar manner among the mutants tested, implying that the observed effects are due mainly to the NDH-1 mutations but not to alteration of the downstream subunits as described previously (22). In contrast, mutations of the negatively charged Glu-138, Glu-140, and Asp-143 had the greatest impact. With regard to the energy-transducing NDH-1 activities, almost total abolishment was observed with E138A, E138D, E140A, E140Q, D143A and D143N.

From the data of the enzymatic activities of NDH-1 of the mutants, we anticipated that Glu-138, Glu-140, and Asp-143 are essential residues. Therefore, we performed further studies on these 3 carboxyl residues.

Contents of peripheral subunits of the mutants of the three essential residues

We analyzed the effect of the mutation on the content of peripheral subunits of *E. coli* NDH-1 membranes. Antibodies against the peripheral subunits NuoB, NuoCD, NuoE, NuoF, NuoG and NuoI were used for this purpose. As seen in Fig. 3, all the peripheral subunits including NuoCD, were entirely missing in membranes of the KO-C mutant. The mutations E138A, E140A and D143A resulted in a significant loss of subunit NuoCD and

nearly all other hydrophilic subunits. In contrast, E140D and D143E substitutions did not affect the content of any of the tested hydrophilic subunits, while mutant E138D had a relatively low content for all the hydrophilic subunits. Replacement of these carboxylic residues by their corresponding amide displayed distinct results. Interestingly, mutants E140Q and D143N showed a significantly lower amount of the peripheral subunits than the wild-type, while in the case of the E138Q mutant the peripheral subunits were relatively high as compared to the above two amide mutants.

Effect of the mutations on subunit assembly of NDH-1 of the mutants of the three essential residues

To directly verify whether mutations in the NuoC segment of the NuoCD subunit affects assembly of NDH-1, we performed BN-PAGE analysis of the mutants Glu-138, Glu-140, and Asp-143 (Fig. 4). The results are mostly in good agreement with the data obtained from the assay of dNADH-$K_3Fe(CN)_6$ reductase activity. As expected, the NDH-1 band was detected for mutants E140D and D143E, suggesting normal subunit assembly in these mutants (Fig. 4). In contrast, mutants E138A, E140A and D143A with almost null ferricyanide activity lacked a NDH-1 band. Mutants that had considerably lower ferricyanide activities displayed no NDH-1 band (E138Q, E138D, E140Q, and D143N). In the case of E138Q, nearly normal amounts of the peripheral subunits were observed in the membranes as described above. It appears that the NDH-1 of mutant E138Q is inactively assembled and is susceptible to the detergent extraction during the BN-PAGE procedure. These data suggest that negative results with BN-PAGE need to be interpreted with caution and may require additional experiments when assessing the assembly of mutanted NDH-1.

Electrochemical Potential and Proton Translocation of the the three conserved carboxyl residues mutants

Next, we have determined the proton translocation ability of membrane vesicles for the three carboxyl residue mutants using ACMA as the fluorescent indicator. In addition, the electrochemical potential (ΔΨ) was monitored by following the absorbance changes of oxonol VI in response to dNADH oxidation (Fig. 5). All activities were dissipated when using the uncoupler FCCP. No ΔΨ was observed for the membrane vesicles of the KO-C mutant. Complete absence of proton translocation and ΔΨ was observed for the alanine mutants of the conserved acidic residues of the α-helix as expected from their lack of NDH-1 assembly. Partial proton translocation was observed in case of E138Q, while almost complete restoration of proton translocation ability was observed for the conserved mutants E140D and D143E (Fig. 5A). Similar trends were seen for the above conserved mutants in the ΔΨ measurements (Fig. 5B). These results indicate that E140D and D143E have normal energy-coupled NADH-Q oxidoreductase activity.

DISCUSSION

The NuoC/Nqo5/30k subunit has a unique presence in the peripheral domain of NDH-1 and complex I. It carries no known cofactor, and no functional role in the catalysis of the enzyme has been identified. What is intriguing is that a counterpart of the NuoC subunit exists in the energy-converting [Ni-Fe] hydrogenase (Ech) from *Methanosarcina barkeri* which consists only of 6 subunits (36). It seems as if NuoC is a member of the "core of the core subunits" which led us to believe it bears a critically important role. Indeed, our present work demonstrated that there are at least three essential amino acids in the NuoC segment of the *E. coli* NuoCD subunit (Glu-138, Glu-140, and Asp-143) whose single point mutation could cause total disruption of the peripheral domain. All three residues are located in the same third α-helix. These highly conserved acidic residues are also conserved in the EchD subunit (^{75}Axxx^{79}Ex^{81}Exx^{84}Dxx^{87}Gxx^{90}F) of *M. barkeri* (36,37) as well as the HycE

subunit of hydrogenase-3 and the HyfG subunit of hydrogenase-4 from *E. coli* (Fig. 2B) (3,38,39).

In the first 3D structural model determined for the peripheral arm of *Thermus* NDH-1 (PDB code: 3FUG) by Sazanov's group, a possible ionic interaction was suggested between the conserved acidic residue Asp-120 of Nqo5 (Asp-143 in *E. coli*) and the C-terminal Arg-409 of Nqo4 (Arg-600 in *E. coli*) (10). In the further refined structural model reported recently by the same group (PDB code: 3IAS) (11), the region around the third helix has been adjusted. In place of Asp-120, another conserved acidic residue Glu-117 (Glu-140 in *E. coli*) is now in close vicinity of Arg-409 (2.8 Å). Glu-117 is also close to Lys-369 of Nqo4 (Arg-560 in *E. coli*) (3.3 Å). When the *E. coli* NDH-1 model was superimposed onto the *Thermus* structural model, a quite similar spatial relationship among the three residues was seen (Fig. S3). Glu-140 of the NuoC segment was 2.7 Å from the C terminal Arg-600 of the NuoD segment and 3.1 Å from Arg-560 of the NuoD segment. It can therefore be speculated that ionic interaction between Glu-140 and the two positively charged residues in the NuoD segment may contribute to the structural integrity of the subunit. In fact, in the *Y. lipolytica* enzyme, mutating the C-terminal Arg-466 (Arg-600 in *E. coli*) to Met was reported to change the ubiquinone affinity and inhibitor sensitivity (40). Our preliminary experiments suggest that the mutation of Arg-560 or Arg-600 of *E. coli* NDH-1 causes partial inhibition of the NADH oxidase activity. Two other essential residues, Glu-138 and Asp-143, do not seem to have a possible ion-pairing partner either in the *Thermus* structural model or in our hypothesized *E. coli* model.

What constitutes the most notable observation in the current work is that the highly conserved Glu-138 and Asp-143 whose replacement led to almost complete destruction of the integrity of the peripheral domain are centered around the third helix (Fig. 2). Glu-140 of this helix may be contributing to the interaction with the NuoD segment as discussed above, but Glu-138 and Asp-143 are located on the outward facing side of the helix. It can be speculated that modification of this area of the molecule might prevent correct folding or appropriate interaction with other subunits. We have previously reported that the NuoH (ND1) subunit of the membrane domain bears a critical role in the assembly of NDH-1 through its cytoplasmic loops (24) in addition to various inhibitor-binding sites (41–46). Among all membrane-domain subunits we have studied, NuoH was the only subunit whose single point mutation resulted in incomplete assembly of NDH-1 (20–24). The longest cytoplasmic loop of NuoH is predicted to be nearly 50 amino acid long. Another interesting piece of information relating to this long loop came from an earlier work with *Paracoccus* NDH-1 in which replacement of a few residues in the loop was shown to alter the kinetic parameters of NADH-Q oxidoreductase activity (47). It is possible that the NuoH subunit, with the loop extending into the peripheral arm, might interact with subunit NuoCD and together serve as a structural support for the entire NDH-1. In fact, our point mutation experiments of NuoH suggest that the conserved charged residues in the four cytoplasmic loops may interact with NuoCD and NuoB (24). In addition to the residues in the NuoC segment studied in the present work, several highly conserved residues are found in the NuoD segment that are seemingly not facing the Q-binding cavity predicted in the *Thermus* NDH-1 structure (Fig. 6A). It is possible that they are involved in the postulated interaction with NuoH. Recently, Sazanov's group reported a 3D structural model of the whole *Thermus* NDH-1 (48). Although the resolution is too low to decipher the atomic structure of the membrane domain, it is clearly seen that the Nqo8/NuoH subunit in the membrane is located almost right beneath the Nqo4+5/NuoCD subunit as if they are forming a central core connecting the two domains (Fig. 6B). We should also point out that the aforementioned 6-subunit Ech from *M. barkeri* contains counterparts of NuoC, NuoD and NuoH (36). Furthermore, it is quite interesting that recent work on the biogenesis of complex I in mitochondria reportedly identified a subcomplex containing the 30k (NuoC) and the ND1

(NuoH) subunits, but not any of the other ND subunits (49). Provided the same synthetic pathway exists for NDH-1, it is conceivable that defects in the 30k (NuoC) subunit might result in a total or partial failure of an assembly of the whole complex, again in agreement with our current work. The speculated subunit-subunit interaction between NuoCD and NuoH remains to be determined experimentally.

In conclusion, through the investigation of highly conserved residues of the NuoC segment in the NuoCD subunit of *E. coli* NDH-1, we have highlighted the role of three highly conserved carboxyl residues (Glu-138, Glu-140, and Asp-143) in the NuoCD subunit in the overall architecture of NDH-1. The key feature includes its potential engagement in the connection between the peripheral domain and the membrane domain providing support for the integrity of the whole enzyme structure.

Supplementary Material

Refer to Web version on PubMed Central for supplementary material.

The abbreviations used are

Q	quinone(s)
complex I	mitochondrial proton-translocating NADH-quinone oxidoreductase
NDH-1	bacterial proton-translocating NADH-quinone oxidoreductase
DB	2,3-dimethoxy-5-methyl-6-decyl-1,4-benzoquinone
dNADH	reduced nicotinamide hypoxanthine dinucleotide (deamino-NADH)
Spc	Spectinomycin
oxonol VI	bis-(3-propyl-5-oxoisoxazol-4-yl) pentamethine oxonol
ACMA	9-amino-6-chloro-2-methoxyacridine
FCCP	carbonyl cyanide-*p*-trifluoromethoxy-phenylhydrazone
MOPS	4-morpholinepropanesulfonic acid
BN-PAGE	blue native-polyacrylamide gel electrophoresis

Acknowledgments

We thank Dr. George M. Church (Harvard Medical School, Boston, MA) for allowing us to use the pKO3 plasmid, Dr. Hideto Miyoshi (Kyoto University, Kyoto) for his kind gift of Capsaicin 40, Drs Byoung Boo Seo and Mathieu Marella (TSRI, La Jolla) for discussion, and Dr. Jennifer Barber-Singh (TSRI, La Jolla) for critical reading of this manuscript.

References

1. Walker JE. The NADH:ubiquinone oxidoreductase (complex I) of respiratory chains. Q. Rev. Biophys. 1992; 25:253–324. [PubMed: 1470679]
2. Yagi T, Matsuno-Yagi A. The proton-translocating NADH-quinone oxidoreductase in the respiratory chain: The secret unlocked. Biochemistry. 2003; 42:2266–2274. [PubMed: 12600193]
3. Brandt U. Energy Converting NADH:Quinone Oxidoreductase (Complex I). Annu. Rev. Biochem. 2006; 75:69–92. [PubMed: 16756485]
4. Carroll J, Fearnley IM, Skehel JM, Shannon RJ, Hirst J, Walker JE. Bovine complex I is a complex of forty-five different subunits. J. Biol. Chem. 2006; 281:32724–32727. [PubMed: 16950771]

5. Yagi T, Yano T, Matsuno-Yagi A. Characteristics of the energy-transducing NADH-quinone oxidoreductase of *Paracoccus denitrificans* as revealed by biochemical, biophysical, and molecular biological approaches. J. Bioenerg. Biomembr. 1993; 25:339–345. [PubMed: 8226715]
6. Yagi T, Yano T, Di Bernardo S, Matsuno-Yagi A. Procaryotic complex I (NDH-1), an overview. Biochim. Biophys. Acta. 1998; 1364:125–133. [PubMed: 9593856]
7. Guénebaut V, Schlitt A, Weiss H, Leonard K, Friedrich T. Consistent structure between bacterial and mitochondrial NADH:ubiquinone oxidoreductase (complex I). J. Mol. Biol. 1998; 276:105–112. [PubMed: 9514725]
8. Ohnishi T. Iron-sulfur clusters semiquinones in Complex I. Biochim. Biophys. Acta. 1998; 1364:186–206. [PubMed: 9593887]
9. Hinchliffe P, Sazanov LA. Organization of iron-sulfur clusters in respiratory complex I. Science. 2005; 309:771–774. [PubMed: 16051796]
10. Sazanov LA, Hinchliffe P. Structure of the Hydrophilic Domain of Respiratory Complex I from *Thermus thermophilus*. Science. 2006; 311:1430–1436. [PubMed: 16469879]
11. Berrisford JM, Sazanov LA. Structural basis for the mechanism of respiratory complex I. J. Biol. Chem. 2009; 284:29773–29783. [PubMed: 19635800]
12. Nakamaru-Ogiso E, Yano T, Yagi T, Ohnishi T. Characterization of the iron-sulfur cluster N7(N1c) in the subunit NuoG of the proton-translocating NADH-quinone oxidoreductase from *Escherichia coli*. J. Biol. Chem. 2005; 280:301–307. [PubMed: 15520003]
13. Nakamaru-Ogiso E, Matsuno-Yagi A, Yoshikawa S, Yagi T, Ohnishi T. Iron-sulfur cluster N5 is coordinated by a HXXXCXXCXXXXXC motif in the nuog subunit of E. coli NADH:Quinone oxidoreductase (complex I). J. Biol. Chem. 2008; 283:25979–25987. [PubMed: 18603533]
14. Friedrich T. The NADH:ubiquinone oxidoreductase (complex I) from *Escherichia coli*. Biochim. Biophys. Acta. 1998; 1364:134–146. [PubMed: 9593861]
15. Dupuis A, Chevallet M, Darrouzet E, Duborjal H, Lunardi J, Issartel JP. The Complex I from *Rhodobacter capsulatus*. Biochim. Biophys. Acta. 1998; 1364:147–165. [PubMed: 9593868]
16. Yano T, Chu SS, Sled' VD, Ohnishi T, Yagi T. The proton-translocating NADH-quinone oxidoreductase (NDH-1) of thermophilic bacterium *Thermus thermophilus* HB-8: Complete DNA sequence of the gene cluster and thermostable properties of the expressed NQO2 subunit. J. Biol. Chem. 1997; 272:4201–4211. [PubMed: 9020134]
17. Darrouzet E, Issartel JP, Lunardi J, Dupuis A. The 49-kDa subunit of NADH-ubiquinone oxidoreductase (Complex I) is involved in the binding of piericidin and rotenone, two quinone-related inhibitors. FEBS Lett. 1998; 431:34–38. [PubMed: 9684860]
18. Prieur I, Lunardi J, Dupuis A. Evidence for a quinone binding site close to the interface between NUOD and NUOB subunits of Complex I. Biochim. Biophys. Acta. 2001; 1504:173–178. [PubMed: 11245783]
19. Kashani-Poor N, Zwicker K, Kerscher S, Brandt U. A central functional role for the 49 kDa subunit within the catalytic core of mitochondrial complex I. J. Biol. Chem. 2001; 276:24082–24087. [PubMed: 11342550]
20. Kao MC, Di Bernardo S, Perego M, Nakamaru-Ogiso E, Matsuno-Yagi A, Yagi T. Functional roles of four conserved charged residues in the membrane domain subunit NuoA of the proton-translocating NADH-quinone oxidoreductase from *Escherichia coli*. J. Biol. Chem. 2004; 279:32360–32366. [PubMed: 15175326]
21. Kao MC, Di Bernardo S, Nakamaru-Ogiso E, Miyoshi H, Matsuno-Yagi A, Yagi T. Characterization of the membrane domain subunit NuoJ (ND6) of the NADH-quinone oxidoreductase from *Escherichia coli* by chromosomal DNA manipulation. Biochemistry. 2005; 44:3562–3571. [PubMed: 15736965]
22. Kao MC, Nakamaru-Ogiso E, Matsuno-Yagi A, Yagi T. Characterization of the membrane domain subunit NuoK (ND4L) of the NADH-quinone oxidoreductase from *Escherichia coli*. Biochemistry. 2005; 44:9545–9554. [PubMed: 15996109]
23. Torres-Bacete J, Nakamaru-Ogiso E, Matsuno-Yagi A, Yagi T. Characterization of the NuoM (ND4) subunit in *Escherichia coli* NDH-1: Conserved charged residues essential for energy-coupled activities. J. Biol. Chem. 2007; 282:36914–36922. [PubMed: 17977822]

24. Sinha PK, Torres-Bacete J, Nakamaru-Ogiso E, Castro-Guerrero N, Matsuno-Yagi A, Yagi T. Critical roles of subunit NuoH (ND1) in the assembly of peripheral subunits with the membrane domain of *Escherichia coli* NDH-1. J. Biol. Chem. 2009; 284:9814–9823. [PubMed: 19189973]
25. Nakamaru-Ogiso E, Kao MC, Chen H, Sinha SC, Yagi T, Ohnishi T. The membrane subunit NuoL(ND5) is involved in the indirect proton pumping mechanism of E. coli complex I. J. Biol. Chem. 2010
26. Finel M. Organization and evolution of structural elements within complex I. Biochim. Biophys. Acta. 1998; 1364:112–121. [PubMed: 9593850]
27. Satoh T, Miyoshi H, Sakamoto K, Iwamura H. Comparison of the inhibitory action of synthetic capsaicin analogues with various NADH-ubiquinone oxidoreductases. Biochim. Biophys. Acta. 1996; 1273:21–30. [PubMed: 8573592]
28. Torres-Bacete J, Sinha PK, Castro-Guerrero N, Matsuno-Yagi A, Yagi T. Features of subunit NuoM (ND4) in *Escherichia coli* NDH-1: Topology and implication of conserved Glu144 for coupling site 1. J. Biol. Chem. 2009; 284:33062–33069. [PubMed: 19815558]
29. Link AJ, Phillips D, Church GM. Methods for generating precise deletions and insertions in the genome of wild-type *Escherichia coli*: application to open reading frame characterization. J. Bacteriol. 1997; 179:6228–6237. [PubMed: 9335267]
30. Amarneh B, Vik SB. Mutagenesis of Subunit N of the *Escherichia coli* Complex I. Identification of the Initiation Codon and the Sensitivity of Mutants to Decylubiquinone. Biochemistry. 2003; 42:4800–4808. [PubMed: 12718520]
31. Schagger H, Von Jagow G. Blue native electrophoresis for isolation of membrane protein complexes in enzymatically active form. Anal. Biochem. 1991; 199:223–231. [PubMed: 1812789]
32. Sali A, Blundell TL. Comparative protein modelling by satisfaction of spatial restraints. J. Mol. Biol. 1993; 234:779–815. [PubMed: 8254673]
33. Larkin MA, Blackshields G, Brown NP, Chenna R, McGettigan PA, McWilliam H, Valentin F, Wallace IM, Wilm A, Lopez R, Thompson JD, Gibson TJ, Higgins DG. Clustal W and Clustal X version 2.0. Bioinformatics. 2007; 23:2947–2948. [PubMed: 17846036]
34. DeLano, WL. The PyMOL Molecular Graphics System. DeLano Scientific LLC. Palo Alto, CA, USA: 2008. http://www.pymol.orgRef Type: Online Source
35. Matsushita K, Ohnishi T, Kaback HR. NADH-ubiquinone oxidoreductases of the *Escherichia coli* aerobic respiratory chain. Biochemistry. 1987; 26:7732–7737. [PubMed: 3122832]
36. Hedderich R. Energy-converting [NiFe] hydrogenases from archaea and extremophiles: ancestors of complex I. J. Bioenerg. Biomembr. 2004; 36:65–75. [PubMed: 15168611]
37. Meuer J, Kuettner HC, Zhang JK, Hedderich R, Metcalf WW. Genetic analysis of the archaeon Methanosarcina barkeri Fusaro reveals a central role for Ech hydrogenase and ferredoxin in methanogenesis and carbon fixation. Proc. Natl. Acad. Sci. USA. 2002; 99:5632–5637. [PubMed: 11929975]
38. Andrews SC, Berks BC, McClay J, Ambler A, Quail MA, Golby P, Guest JR. A 12-cistron *Escherichia coli* operon (hyf) encoding a putative proton-translocating formate hydrogenlyase system. Microbiology. 1997; 143(Pt 11):3633–3647. [PubMed: 9387241]
39. Friedrich T. Complex I: a chimaera of a redox and conformation-driven proton pump? J. Bioenerg. Biomembr. 2001; 33:169–177. [PubMed: 11695826]
40. Grgic L, Zwicker K, Kashani-Poor N, Kerscher S, Brandt U. Functional significance of conserved histidines and arginines in the 49 kDa subunit of mitochondrial complex I. J. Biol. Chem. 2004; 279:21193–21199. [PubMed: 15004020]
41. Earley FGP, Patel SD, Ragan CI, Attardi G. Photolabelling of a mitochondrially encoded subunit of NADH dehydrogenase with [^{3}H]dihydrorotenone. FEBS Lett. 1987; 219:108–113. [PubMed: 3297786]
42. Earley FG, Ragan CI. Photoaffinity labelling of mitochondrial NADH dehydrogenase with arylazidoamorphigenin, an analogue of rotenone. Biochem. J. 1984; 224:525–534. [PubMed: 6517863]
43. Yagi T, Hatefi Y. Identification of the DCCD-binding subunit of NADH-ubiquinone oxidoreductase (complex I). J. Biol. Chem. 1988; 263:16150–16155. [PubMed: 3141400]

44. Schuler F, Casida JE. Functional coupling of PSST and ND1 subunits in NADH:ubiquinone oxidoreductase established by photoaffinity labeling. Biochim. Biophys. Acta. 2001; 1506:79–87. [PubMed: 11418099]
45. Sekiguchi K, Murai M, Miyoshi H. Exploring the binding site of acetogenin in the ND1 subunit of bovine mitochondrial complex I. Biochim. Biophys. Acta. 2009; 1787:1106–1111. [PubMed: 19265669]
46. Kakutani N, Murai M, Sakiyama N, Miyoshi H. Exploring the Binding Site of Deltalac-Acetogenin in Bovine Heart Mitochondrial NADH-Ubiquinone Oxidoreductase. Biochemistry. 2010; 49:4794–4803. [PubMed: 20459120]
47. Kurki S, Zickermann V, Kervinen M, Hassinen I, Finel M. Mutagenesis of Three Conserved Glu Residues in a Bacterial Homologue of the ND1 Subunit of Complex I Affects Ubiquinone Reduction Kinetics but Not Inhibition by Dicyclohexylcarbodiimide. Biochemistry. 2000; 39:13496–13502. [PubMed: 11063586]
48. Efremov RG, Baradaran R, Sazanov LA. The architecture of respiratory complex I. Nature. 2010; 465:441–445. [PubMed: 20505720]
49. Perales-Clemente E, Fernandez-Vizarra E, Acin-Perez R, Movilla N, Bayona-Bafaluy MP, Moreno-Loshuertos R, Perez-Martos A, Fernandez-Silva P, Enriquez JA. Five Entry Points of the Mitochondrially Encoded Subunits in Mammalian Complex I Assembly. Mol. Cell Biol. 2010; 30:3038–3047. [PubMed: 20385768]
50. Laemmli UK. Cleavage of structural proteins during the assembly of the head of bacteriophage T4. Nature. 1970; 227:680–685. [PubMed: 5432063]

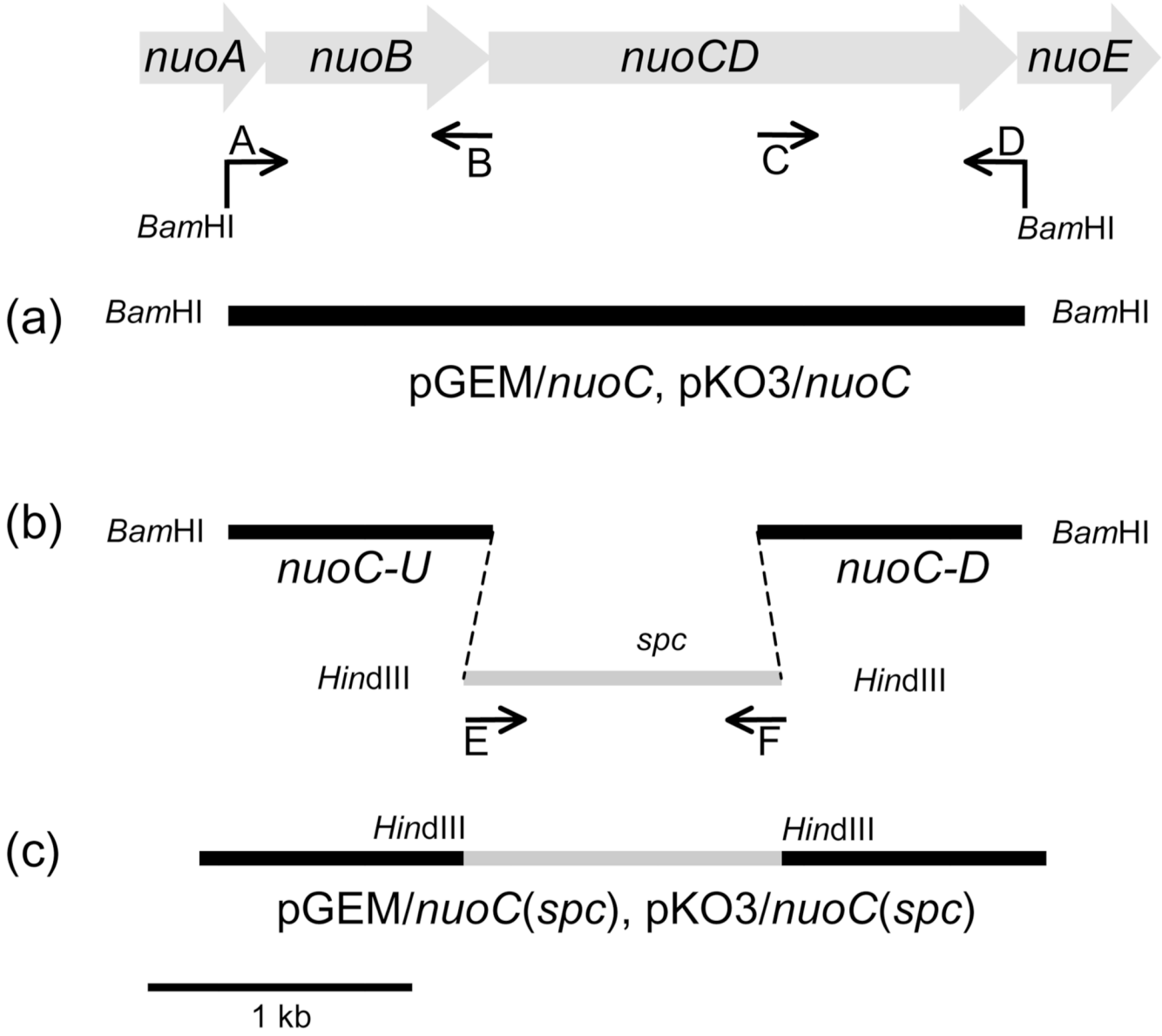

Figure 1.

Schematic representation of the strategy for *nuoC* segment cloning, insertion of a *spc* cassette in the *E. coli nuoCD* gene and the construction of site-specific NuoC segment mutants. In this work, we selected the part of *nuoCD* gene that codifies the homologous segment of the Nqo5 from *T. thermophilus* (NuoC). Arrows indicate the primers used in this study. (a) Amplified product *nuoC*+1 kb upstream +1 kb downstream (*NuoC*) was cloned in pGEM-T Easy vector and subcloned into the vector pKO3 resulting in plasmids named pGEM/*nuoC* and pKO3/*nuoC*, respectively. (b) The spectinomycin-encoding gene (*spc*) was obtained by using the primers E and F, both containing the *Hind*III restriction site. (c) *spc* was cloned in pGEM-T Easy vector and inserted between the fragments *nuoC-U* and *nuoC-D* utilizing the *Hind*III restriction sites and finally assembled in the pKO3 vector (pKO3/*nuoC* (*spc*)) with the help of *Bam*HI restriction sites.

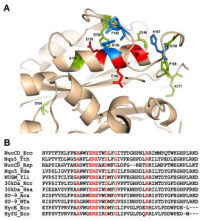

Figure 2.

Structural analyses near the third α-helix of the *E. coli* NuoC segment. (A): Proposed 3D model for the interface area of NuoC and NuoD segments of the *E.coli* NuoCD subunit. The 3D model was obtained for *E. coli* by homology modeling based on the crystallographic data of the *T. thermophilus* enzyme (10) using MODELLER 9v8 software. Visualization was made with PyMOL v1.2 (32). (B): Comparison of primary sequence in and near the third α-helix of the NuoC segment between the *E. coli* NuoCD and its homologs. NuoCD_Eco, *E. coli* NuoCD *(NP_416789);* Nqo5_Tth, *T. thermophilus* Nqo5 *(YP_005887.1);* NuoCD_Rsp, *R. sphaeroides* NuoC *(YP_3531178.1);* Nqo5_Pde, *Paracoccus denitrificans* Nqo5 *(YP_916036.1);* NUGM_Yli, *Yarrowia lipolytica* NUGM *(XP_504891.1);* 30kDa_Ncr, *Neurospora crassa* 30kDa *(XM_952596.2);* 30kDa_Hsa, *Homo sapiens* 30kDa (NDUFS3) *(NP_004542.1);* SU-9_Aca, *Acanthamoeba castellanii* SU-9 *(NP_042560.1)*; SU-9_Nta, *Nicotiana tabacum* SU-9 *(YP_173479.1)*, HycE_Eco, HycE from *E. coli* hydrogenase-3 (*NP_417201.1*); HyfG_Eco, HyfG from *E. coli* hydrogenase-4 (*NP_416982.1*). The conserved residues are marked in red.

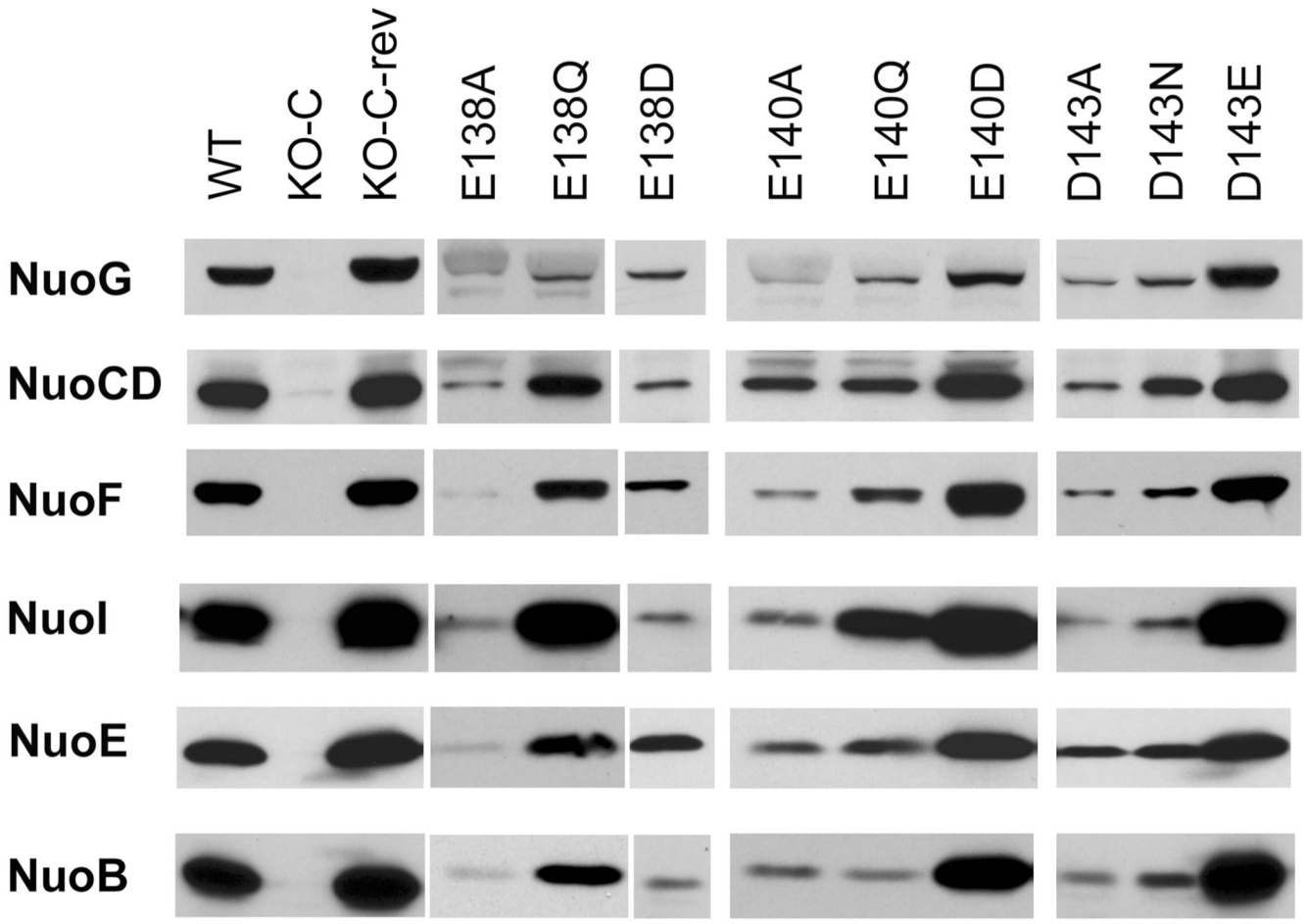

Figure 3.
Western blots using antibodies corresponding to the 6 peripheral subunits (NuoB, NuoCD, NuoE, NuoF, NuoG and NuoI) of membrane preparations from mutants of Glu-138, Glu-140, and Asp-143. *E. coli* membranes (10 μg of protein per lane) were loaded on 10 – 15 % Laemmli SDS-PAGE (50).

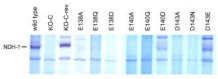

Figure 4.

Effect of mutating the three most conserved carboxyl residues on *E. coli* NDH-1 assembly. BN-PAGE gels from membranes of *E. coli* were stained for NADH dehydrogenase activity. Comparison of wild type, NuoC segment knock-out (KO-C), revertant (KO-C-rev) and some of NuoC segment mutants is shown. The location of NDH-1 band is marked on the left.

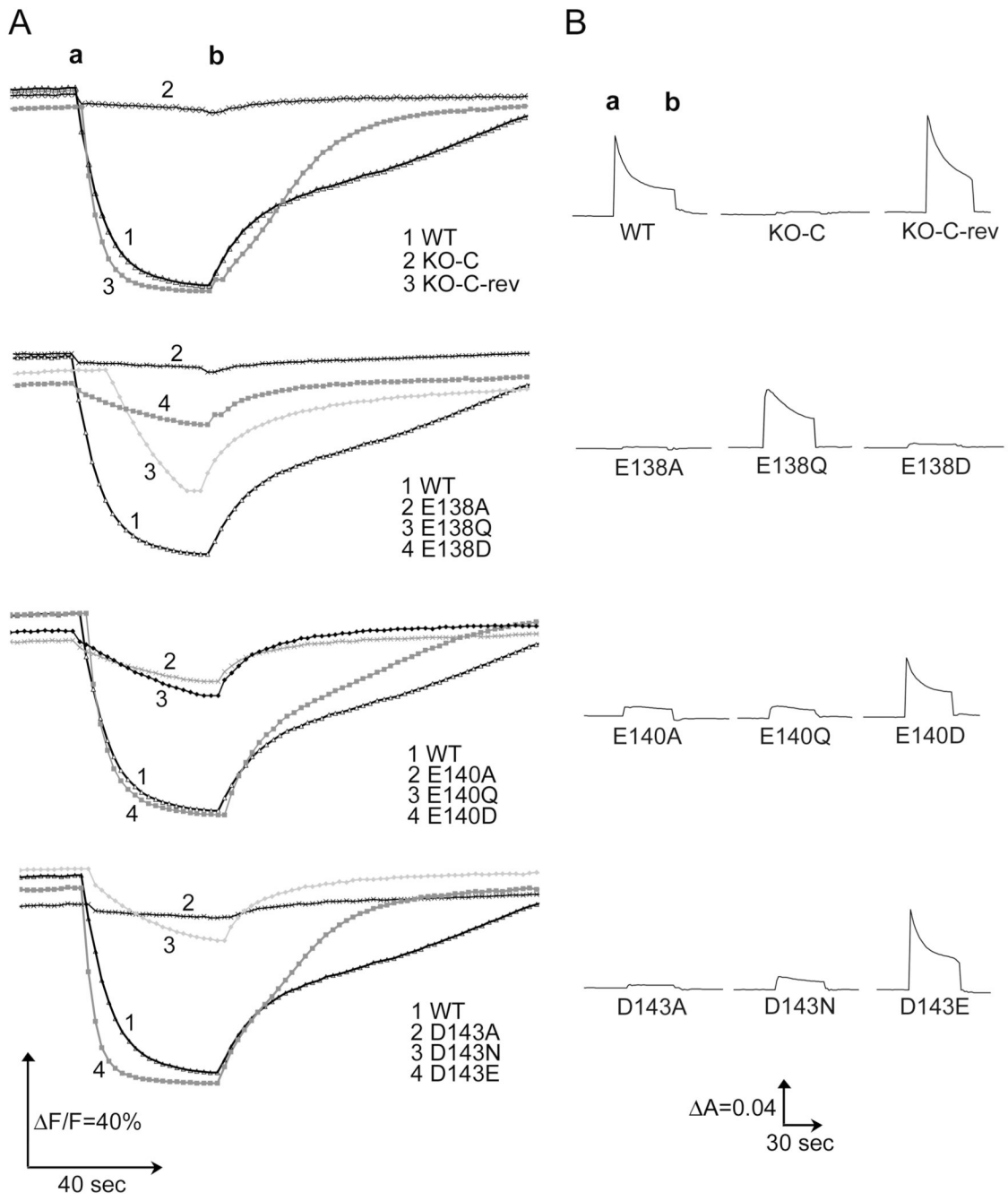

Figure 5.

Effects of mutations of Glu-138, Glu-140, and Asp-143 on proton translocation and membrane potential generated by dNADH oxidase activity in the *E. coli* membrane vesicles. (A): Generation of pH gradient (ΔpH) generated by dNADH oxidation in *E. coli* membrane preparations of wild type and mutants of the three acidic conserved residues in the NuoC segment of the NuoCD subunit. ΔpH was monitored by the quenching of the fluorescence of ACMA at room temperature. Wavelength of 410 (excitation) and 480 (emission) were used. 0.2 mM of dNADH was added as substrate (*a*) or 2 μM of FCCP (*b*) as uncoupler to dissipate the gradient. The assay mixture was constituted of 50 mM MOPS (pH 7.3), 10 mM $MgCl_2$, 50 mM KCl, 2 μM ACMA and 150 μg of protein/ml. (B): Detection of the

membrane potential change ($\Delta\Psi$) generated by dNADH oxidation in *E. coli* membrane preparations for wild type and NuoCD mutants. $\Delta\Psi$ was monitored on membrane samples (330 μg of protein/ml) by the absorbance change at 630-603 nm at 30 °C using oxonol VI as reporter. The assay mixture contained 50 mM MOPS (pH 7.3), 10 mM $MgCl_2$, 50 mM KCl, 2 μM oxonol VI. Addition of 0.2 mM dNADH (*a*) or 2 μM of FCCP (*b*) were made to the reaction mixture.

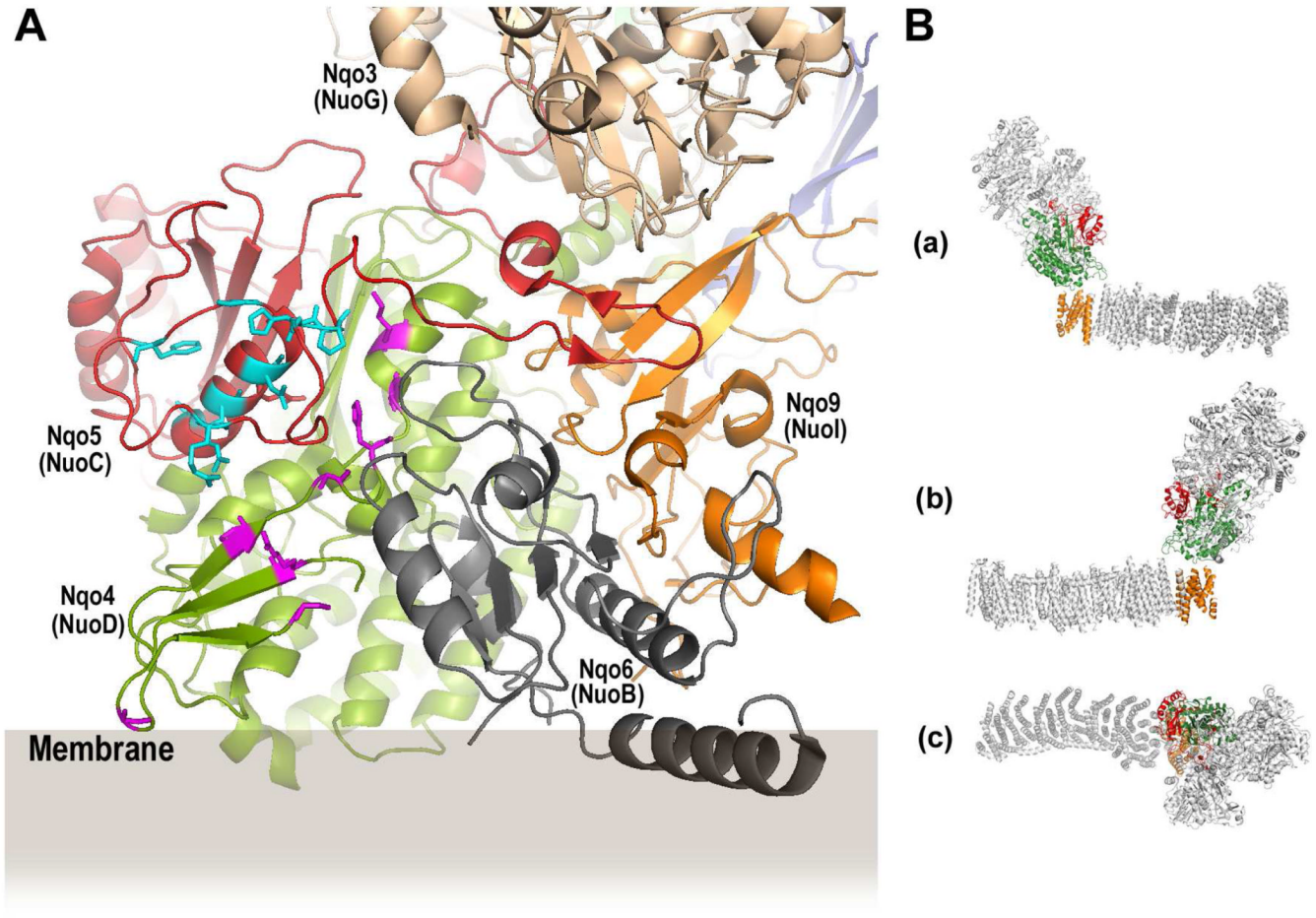

Figure 6.

A: A cartoon representation of part of the peripheral domain of the *Thermus* NDH-1 (PDB: 3IAS) showing highly conserved amino acid residues located in subunits Nqo4 and Nqo5. The *E. coli* naming of the subunits is given in parenthesis. An approximate position of the membrane is drawn according to Berrisford and Sazanov (11). The amino acid residues in Nqo5 highlighted in cyan correspond to the conserved residues in the NuoC segment of *E. coli* NuoCD studied in the current work. The amino acid residues in Nqo4 highlighted in magenta indicate highly conserved residues that are located on or near the surface of the molecule on the same side as the conserved residues in Nqo5.

B: A cartoon representation of *Thermus* NDH-1 (PDB: 3M9S) consisting of the peripheral arm and the transmembrane domain (48) highlighting the three "core of the core subunits", namely, Nqo5/NuoC/30k (red), Nqo4/NuoD/49k (green) and Nqo8/NuoH/ND1 (orange). (a) and (b) are side views; (c) is a top view.

Biochemistry. Author manuscript; available in PMC 2011 November 30.

Table 1

Enzyme activities of the *E. coli* MC4100 NDH-1 and various NuoC segment mutants

	Strain	dNADH-$K_3Fe(CN)_6$ activity[a]	%	dNADH oxidase activity[b]	%	dNADH-DB activity[b]	%
	Wild type	1816 ± 8	100	659 ± 6	100	636 ± 41	100
	KO-C	662 ± 9	36	6 ± 1	1	16 ± 2	3
	KO-C-rev	1746± 64	96	831 ± 22	126	674 ± 58	106
	E138A	890 ± 49	49	11 ± 1	2	18 ± 4	3
	E138Q	798 ± 14	44	134 ± 8	20	185 ± 7	29
	E138D	925 ± 41	51	29 ± 1	4	41 ± 2	6
	E140A	763 ± 26	42	32 ± 3	5	43 ± 1	7
	E140Q	604 ± 6	33	45 ± 10	7	68 ± 12	11
	E140D	1718 ± 63	94	562 ± 1	85	664 ± 32	104
	D143A	903 ± 28	50	10 ± 5	2	22 ± 3	3
	D143N	1252 ± 40	69	36 ± 1	5	58 ± 3	9
	D143E	1863 ± 12	103	868 ± 11	132	816 ± 14	128
	S104A	1870 ± 17	103	699 ± 1	106	727 ± 15	114
	A134S	1489 ± 92	82	n.d.		n.d.	
	R139A	1579 ± 12	87	671 ± 9	102	752 ± 17	118
	G146A	1856 ± 3	102	771 ± 3	117	724 ± 17	114
	F149A	1979 ± 68	109	n.d.		n.d.	
	R156A	2250 ± 1	124	864 ± 5	131	781 ± 29	123
	G166A	2061 ± 24	113	868 ± 7	132	741 ± 19	117
	H167A	1683 ± 16	93	485 ± 6	74	614 ±13	97
	P168A	1652 ± 68	91	494 ± 33	75	534 ± 53	84
	K171A	1385 ± 14	76	466 ± 12	71	508 ± 3	80
	K171R	1455 ± 17	80	515 ± 3	78	557 ±9	88
	P182A	1819 ± 16	100	470 ± 10	71	560 ± 68	88

[a] Activity in nmol of $K_3Fe(CN)_6$ reduced/mg of protein/min

[b] Activity in nmol of dNADH oxidized/mg of protein/min

n.d., not determined.